Classical tests for statistical evaporation at 680 MeV ^{40}Ar+ ^{nat}Ag

C. J. Gelderloos,[1,2,*] John M. Alexander,[1] J. Boger,[1,†] M. T. Magda,[1] A. Narayanan,[1,‡] P. A. DeYoung,[2] A. Elmaani,[1,§] and M. A. McMahan[3]

[1]*Departments of Physics and Chemistry, State University of New York at Stony Brook, Stony Brook, New York 11794*

[2]*Department of Physics, Hope College, Holland, Michigan 49423*

[3]*Lawrence Berkeley Laboratory, 1 Cyclotron Road, Berkeley, California 94720*

(Received 11 July 1996)

Measurements of the partial linear momentum transfer and production cross sections for light charged particles are reported for the reaction 680 MeV ^{40}Ar+^{nat}Ag. From examination of light charged particle invariant cross section maps and comparison of experimental angular distributions and energy spectra to a reaction kinematics simulation, an average value of 85% linear momentum transfer is deduced, with a spin range of $(0–75)\hbar$. Integration over energy and angle yields single and coincident light charged particle production cross sections. [S0556-2813(96)02812-9]

PACS number(s): 25.70.Gh

I. INTRODUCTION

Heavy-ion collisions provide the primary experimental method used to study energy dissipation in hot nuclei. The extent to which nuclei can contain and distribute internal excitation energy among their constituents is of great interest for elucidating nuclear properties and reaction mechanisms. For bombarding energies less than 10*A* MeV, central collisions in the ^{40}Ar+^{nat}Ag reaction involve predominantly complete fusion of projectile and target [1,2]. This complete fusion process leads to the formation of an equilibrated compound-nucleus emission source for the light charged particles (LCP's) and neutrons. Large angle LCP coincidences provide information on the equilibration and angular momentum of the source [1].

At bombarding energies of 17*A* MeV, studies of small angle correlations indicate that the lifetimes of composite sources decrease substantially from that of 8*A* MeV [3–5]. In the context of the statistical model, a shortening of lifetimes for particle emission is indicative of increasing excitation energy. In order for these lifetimes to be reliable, the source of the emitted LCP's must be properly characterized, especially since evidence for partial linear momentum transfer has been previously noted in other systems ([6], e.g.). An extensive set of publications exists which studies the ^{40}Ar+^{nat}Ag system for bombarding energies of $7A–34A$ MeV, providing much detailed information about source characteristics [7–17]. These studies portray a predominantly equilibrated system emitting many charged particles during the deexcitation chain. The excitation energy of the composite system continues to increase as a function of bombarding energy. Evidence for partial linear momentum transfer has been noted via two different methods: measurement of the fission folding angle [10] and residue velocity spectra [14,17].

This paper uses the detailed analysis of LCP emission patterns to deduce linear momentum transfer (LMT), multiplicities, and spin range of a composite emitter. LCP's have been used extensively to probe the nature and extent of equilibration. Symmetry about 90° in the emitter frame in LCP angular distributions is an effective indication of thermalization [18]. Coincident LCP measurements provide significant additional constraints on the angular momentum extracted by comparison to kinematic simulations. Furthermore, detailed examination of energy spectra yields accurate information on source velocity, as well as angular momentum, excitation energy, and empirical LCP emission barriers. These techniques, used in conjunction with one another, are used in this paper to extract a detailed picture of reaction dynamics, complementary to previous studies.

II. EXPERIMENTAL DETAILS

The experiment was conducted at the 88-Inch Cyclotron at Lawrence Berkeley Laboratory. A schematic diagram of the reaction chamber configuration is shown in Fig. 1. Three types of detector telescopes were used. Solid state telescopes (SST's) consisting of three segments of silicon surface-barrier detectors were placed at 65°, 85°, and 155° polar angles. Each telescope was comprised of silicon detectors of thickness ≈50, 500, and 5000 μm. Single-element gas ionization chambers (GT's), consisting of a ΔE gas section preceding a 300 μm silicon detector, were placed at 25° and 45° in plane and 45° out of plane (OOP) above the beam. Two wedge detectors [19], consisting of five silicon detectors each, with thicknesses of 500 μm to 3 mm, spaced 10° apart, and sharing a common ΔE gas ionization chamber, were placed spanning polar angles of 65°–105° and 115°–155°. The gas sections of the wedges and GT's were maintained at pressures of 20 and 40 torr isobutane, respectively. Each had an active length of ≈5 cm. Both wedges and GT's detected alpha particles and intermediate mass fragments

*Present address: Nuclear Physics Laboratory, University of Colorado, Boulder, Colorado 80309-0446.

†Present address: Department of Chemistry, Brookhaven National Laboratory, Upton, New York 11973.

‡Present address: United Nations Development Program, 55 Lodi Estate, New Delhi 110003 India.

§Present address: Battelle Pacific Northwest National Laboratory, Richland, Washington 99352.

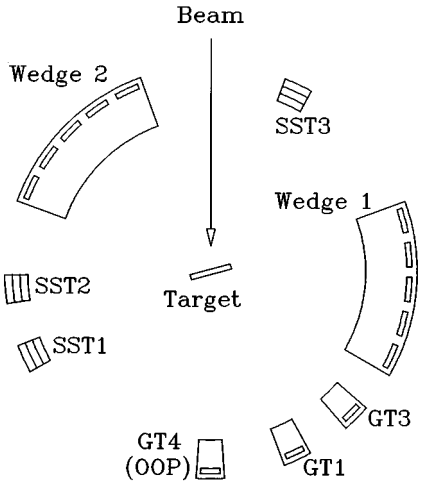

FIG. 1. A schematic diagram of the detector configuration within the reaction chamber is depicted. Abbreviations and descriptions of the detectors are given in the text.

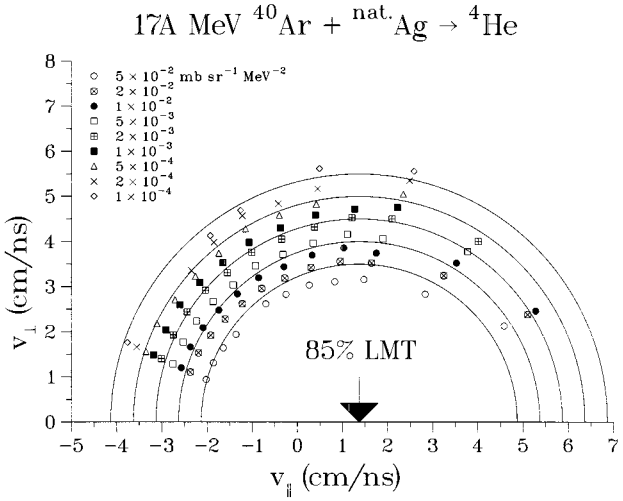

FIG. 2. An invariant cross-section map for inclusive alpha particles is shown. Data are represented by points corresponding to labeled values of the invariant cross section. Arcs are drawn centered on a source velocity of 85% full momentum transfer and are provided for comparison to data.

(IMF's), while the SST's detected protons, deuterons, tritons, and alpha particles.

Detectors were placed in a large scattering chamber of approximately 1 m diameter (the Polish chamber). Detectors on either side of the beam were mounted on separate tables which were rotated to provide consistency checks between detectors. Solid angles subtended by each detector were measured in three ways: by geometrical measurement, by radioactive sources of known activity, and by elastic scattering. All three methods were in good agreement, with the geometrical and source measurements giving consistent agreement of less than 5% variation. Typical solid angles were $\approx$1.5 msr for the GT's and $\approx$5 msr for each SST and wedge element. A natural silver target of 0.932 mg/cm^2 areal density was used throughout the experiment. The target thickness was measured by Rutherford scattering and by weighing; both methods yielded consistent results. Corrections for energy loss in the target were made.

Energy calibrations were made by means of radioactive sources and the elastic scattering of low energy nitrogen, neon, and argon beams generated via the ''cocktail'' method developed at LBL [20]. This calibration procedure provides energy markers in a range extending from 3 to 50 MeV, thus alleviating typical uncertainties stemming from a long extrapolation of the calibration line from a few low energy points. Coincidences were recorded for particles from several beam bursts for the purpose of evaluating the contribution of random or uncorrelated coincidences. Experimental data were written to 8 mm magnetic tape and analyzed off line.

III. STUDIES OF LINEAR MOMENTUM TRANSFER

Several systematic studies have noted the increasing role of partial linear momentum transfer (LMT) in central collisions between nuclei at bombarding energies greater than $\approx 10A$ MeV [6, 7, 21–23, for example]. The most direct method of determining the degree of LMT is to measure the velocity distribution of the heavy residual nuclei. While this method is the most intuitive, it is by no means unique in its capability to determine source velocity.

Invariant cross-section maps are commonly used to characterize the velocity of an emitting source or sources [24, for example]. The invariant cross section is defined as

$$\left[\frac{1}{pc}\frac{d^2\sigma}{d\Omega d\epsilon}\right]_{\rm lab}.$$

When there is only one isotropically emitting source, constant values of the invariant cross section lie on a circle centered at the source velocity when plotted as a function of the parallel and perpendicular velocities of the detected particle. Deviations from this isotropic pattern can indicate anisotropies in the particle emission, prethermal emission in the forward direction, or even multiple sources as for peripheral collisions. An invariant cross-section map for inclusive alpha particles is plotted in Fig. 2. Data are shown as points and the arcs are drawn centered on a source velocity of 85% of the center-of-mass velocity of the composite system ($\approx$1.31 cm/ns). This figure provides a qualitative overview of an emission pattern for alpha particles in which the data are reasonably represented by an emitter of velocity 85% LMT. Departures from an isotropic pattern reveal anisotropy about 90° in the emitter frame, as expected from a rotating source (see Fig. 3). Note also the forward peaking of the cross section at 25° and 45° in the laboratory, attributable to prethermal emission.

The qualitative nature of conclusions based on invariant cross-section maps limits their effectiveness in providing a clear picture of reaction dynamics. Much more detailed and quantitative information can be gleaned by close examination of energy spectra and angular distributions. Observations of the sensitivity to such properties as partial linear momentum transfer are facilitated by the use of a kinematic simulation. To this end, the simulation code GANES was employed to provide comparisons to data. The simulation GANES [25] is an extensively tested two-step model which simulates the emission of light charged particles from a highly excited, rapidly rotating source. Energy spectra and angular distributions are fitted empirically by varying the

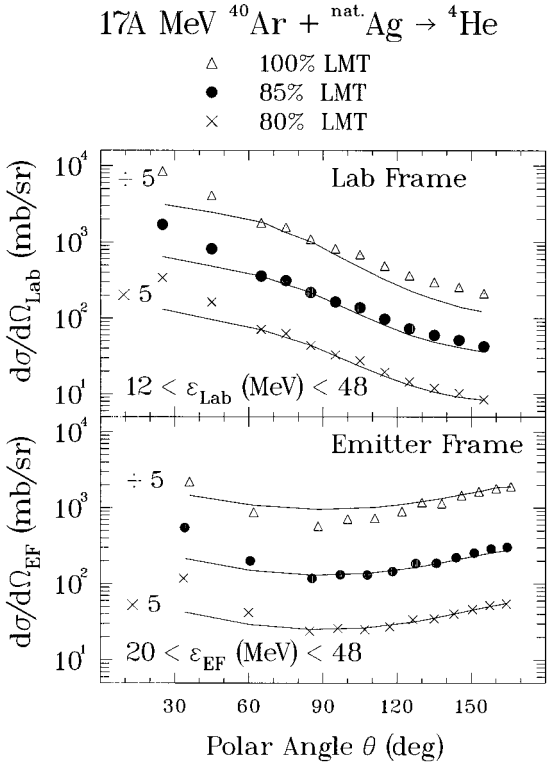

FIG. 3. Angular distributions with various assumptions of linear momentum transfer (LMT) are shown in both laboratory and emitter frames for the inclusive detection of alpha particles. Data are shown as points; GANES calculations are shown as solid curves. A value of 85%±5% LMT is inferred, with an anisotropy of ≈2.6.

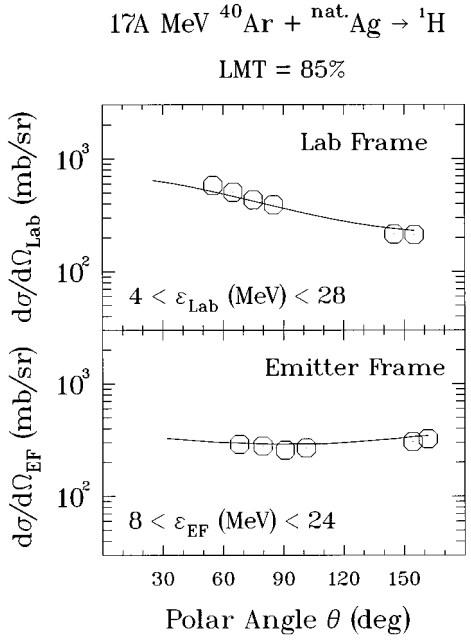

FIG. 4. Angular distributions for protons detected in singles in both laboratory and emitter frames are shown. Open circles represent the data; solid curves represent GANES calculations.

spin range and a fractional energy loss parameter. The fractional energy loss parameter determines an average excitation energy of an effective compound nucleus at the time of emission of the two particles of interest. It is used to characterize the effects of a finite emission chain in which particles are emitted over a range of excitation energies. High quality fits can be obtained for an assortment of experimental observables. The quality of fit is also dependent on the velocity of the emitting source; hence, detailed comparisons of simulation calculations and data provide a basis for determining the LMT.

Figure 3 shows inclusive alpha particle polar angular distributions in both laboratory and emitter frames. The results of several simulation calculations in which the spin range and fractional energy loss are held constant while the emitter velocity is varied are drawn as solid curves. Overall, angular distributions in the emitter frame exhibit a pattern typically associated with the emission of particles from a composite nuclear spinning source, namely, anisotropy about a minimum at $\theta_{EF}=90°$. The calculated angular distributions, shown by the solid curves, vary as a function of LMT. Comparison to data indicates a partial LMT of 85%±5%. This value is in general agreement with other published measurements using various techniques [14, 17, 26, for example].

IV. CHARACTERIZATION OF LIGHT CHARGED PARTICLE EMISSION

Both single and coincident light charged particle data were collected. By analyzing the results with the aid of simulations, a picture emerges of a largely thermalized rotating emitter. For both protons and alpha particles emitted either singly or in coincidence, comparisons with GANES calculations imply an average fractional energy loss of ≈0.5 prior to emission and an angular momentum range of (0–75)$\hbar$. This value of average fractional energy loss implies an average emitter mass of 124 amu, assuming an average of 12 MeV is carried away per emitted nucleon. This is consistent with other measurements of emitter mass [11]. Barriers were empirically chosen as 4.0 and 11.0 MeV for protons and alphas, respectively. A best fit of 85% LMT is indicated by comparison to simulation calculations. These parameters yield the best overall correspondence between data and simulation to a large set of observables. A sample of these comparisons is shown in the figures of this section.

Figure 4 shows angular distributions in both laboratory and emitter frames for protons detected in singles. Data are drawn as open circles and the results of GANES calculations are shown as solid curves. The distribution is nearly isotropic in the emitter frame, with an anisotropy of 1.3. Protons are not strongly constrained by the angular momentum of the emitter and therefore do not reflect the anisotropy that characterizes the emission of heavier particles. The associated energy spectra are shown in Fig. 5. Simulation calculations reproduce the measurements in both spectral shape and intensity as shown by the solid curves. A single normalization factor is used for all calculated energy spectra. For protons there is only a slight hint of a forward-peaked contribution at the smallest polar angles.

Coincidence data are also well characterized by the assumption of an equilibrated rotating source. Figure 6 shows a series of angular distributions of coincidences between two alpha particles with various trigger conditions. Both in-plane and out-of-plane (OOP) triggering was used. GANES simulation results for each angle are plotted as an ''×.'' Several observations can be made about Fig. 6. Isotropy is exhibited

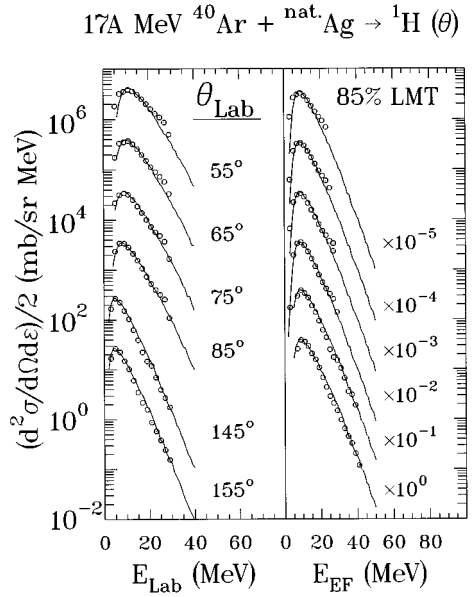

FIG. 5. Energy spectra for protons detected in singles are shown in both the laboratory and emitter frames. GANES calculations are shown as solid curves.

by the in-plane coincidence angular distributions in the emitter frame for polar angles greater than ≈90° (open and solid circles in the lower plot). This isotropy in the backward hemisphere suggests emission from a thermalized source whose angular momentum vector is constrained nearly perpendicular to the emission plane. The requirement of two particles detected in plane is sufficient to significantly restrict

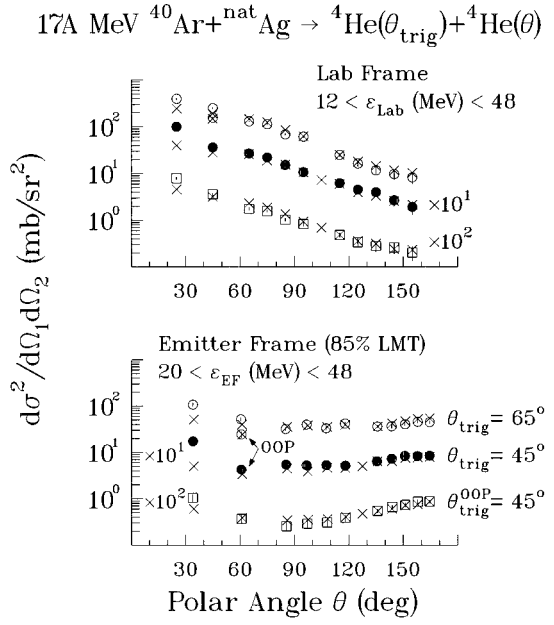

FIG. 6. Angular distributions for two alpha particles detected in coincidence are plotted in laboratory and emitter frames. Results from three different triggering conditions are plotted: open circles denote coincidences triggered by the detection of an alpha particle at $\theta_{lab}=65°$ in plane, solid circles at $\theta_{lab}=45°$ in plane, and open squares at $\theta_{lab}=45°$ out of plane. Each × denotes simulation results.

the direction of the angular momentum vector. For alpha particles detected in singles the angular distributions exhibit an inherent anisotropy (see Fig. 3). This reflects the lack of restriction on the direction of the angular momentum vector when only one alpha particle is detected (i.e., the emission plane is not known); thus, classically the angular momentum vector can lie anywhere in a plane perpendicular to the beam. In the context of the statisitical model, the emission width $d\Gamma$ is

$$d\Gamma \propto \exp(\beta_2 \sin^2\phi),$$

where ϕ is the angle between the emission direction of the particle and the angular momentum vector, and β_2 is the ratio of the rotational energy and the temperature [25, 27, and references therein]. This emission width indicates that the maximum emission probability is in directions perpendicular to the angular momentum vector. The summation of contributions from all possible orientations of the angular momentum vector results in an enhancement in the probability of an alpha being detected in either the forward or backward directions. The detection of the first alpha at a sideward angle in the emitter frame, however, restricts the direction of the angular momentum, enhancing the likelihood that subsequent particle emission is in the same plane. Thus, in-plane emission is nearly isotropic, having no preferred direction. The cross section for the detection of the second alpha particle out of plane is reduced due to the restrictions imposed by the direction of the angular momentum. This is first seen by noting the two points labeled ''OOP'' in the lower plot of Fig. 6, near a polar angle of 60°. A more revealing effect of out-of-plane coincidences is seen in the distribution denoted by open squares in the lower plot, labeled $\theta^{OOP}_{trig}=45°$, in which the trigger alpha particle is detected at 45° out of plane. There is more anisotropy exhibited in this distribution than in the in-plane distributions; the in-plane distribution triggered at 45° (65°) has an anisotropy of 1.6 (1.3), whereas the out-of-plane distribution has an anisotropy of 3.2. The larger out-of-plane anisotropy is as expected for an emitter whose angular momentum is not aligned perpendicular to the plane of the detectors. Application of the kinematical simulation GANES allows for reproduction of in-plane isotropies and out-of-plane anisotropies for a proper choice of the emitter angular momentum. The anisotropy in the out-of-plane distribution provides a stringent constraint on the spin range of the emitter. The agreement between simulation and data indicates that a spin range of $(0–75)\hbar$ is a good characterization.

Simulated coincident energy spectra also constrain the assumed angular momentum of the emitter, since the particle energy is enhanced by the spin-off energy from the rotating source. Figure 7 shows energy spectra for alpha particles triggered by the detection of another alpha particle at $\theta_{lab}=65°$ in the laboratory. Good agreement is shown between simulation calculations and data, especially at backward angles. (Note that the inability of the statistical model to predict the broadening of the spectra at low energies is epidemic [1, e.g.].) Similar agreement is exhibited for energy spectra triggered by the detection of an alpha particle at 45° in or out of plane. Such broad agreement in many observables gives confidence in the characterization of the composite system.

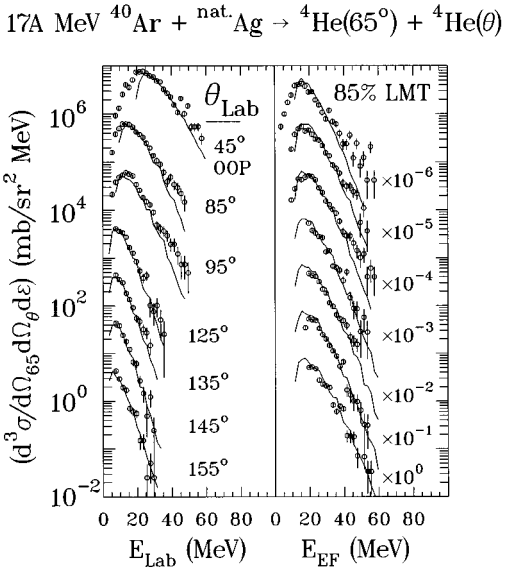

FIG. 7. Energy spectra for coincident alpha particles triggered by the detection of one of the particles at $\theta_{\rm lab}=65°$ in plane are shown in laboratory and emitter frames. Points denote data; solid curves show the results of simulation calculations.

Angle-integrated cross sections for evaporative single and coincident light charged particle production have also been calculated. Values are shown in Table I. Only statistical errors are shown; due to the detailed knowledge of detector solid angles, however, systematic errors are estimated to be small, $\lesssim$15%. These values show general consistency to $\sim$25% with other published values [5]. From the study of multiplicity distributions from the AMPHORA 4π detector, Magda *et al.* [8] have concluded that there is a central collision group of reactions (with a cross section of $\sim$2 b) that emit H and He with an average multiplicity $\langle m_{\rm H,He}\rangle=8.5$. In a more recent study [17] this group found that the reactions with the largest LCP multiplicities were associated with evaporationlike residues with $\langle m_{\rm H,He}\rangle$ values of $\sim$8 from evaporationlike emission and $\sim$2 from forward-peaked emission. From the present study of the singles and coincidence cross sections (Table I) one can use the procedure of Ref. [1] to calculate that the hard central collisions have a subset cross section σ_A of 1.5 ± 0.1 b with $\langle m_{\rm LCP}\rangle=8.4\pm0.5$ for evaporationlike emission. The individual average multiplicities for evaporationlike H and He particles are $\langle m_p\rangle=3.6$, $\langle m_d\rangle=0.8$, $\langle m_t\rangle=0.4$, and $\langle m_\alpha\rangle=3.7$ (each with a standard deviation of $\sim$15%).

TABLE I. Angle-integrated light charged particle cross sections for singles and coincidences in 17*A* MeV ^{40}Ar+$^{\rm nat}$Ag reactions. All numbers are given in units of barns. Uncertainties shown are statistical only.

Single-particle cross sections (b)	
σ_p	5.69 ± 0.02
σ_d	1.13 ± 0.01
σ_t	0.501 ± 0.004
σ_α	6.24 ± 0.03
Particle-particle cross sections (b)	
σ_{pp}	18.2 ± 0.5
σ_{pd}	3.84 ± 0.12
σ_{pt}	1.79 ± 0.08
$\sigma_{p\alpha}$	19.5 ± 0.5
σ_{dd}	0.891 ± 0.075
σ_{dt}	0.356 ± 0.033
$\sigma_{d\alpha}$	4.65 ± 0.16
σ_{tt}	0.091 ± 0.023
$\sigma_{t\alpha}$	2.26 ± 0.10
$\sigma_{\alpha\alpha}$	16.9 ± 0.6

V. CONCLUSIONS

Evidence is provided for light charged particle emission from a predominantly thermalized source with an angular momentum of $(0–75)\hbar$. Energy spectra and angular distributions for light charged particles detected singly and in coincidence are well described by a two-step model, assuming a linear momentum transfer of 85% of the projectile momentum and an average fractional energy loss of approximately half of the available excitation energy before emission. Calculated multiplicities from angle-integrated cross sections are in excellent agreement with 4π measurements of the same reaction.

Financial support has been provided by the U.S. Department of Energy and the National Science Foundation.

[1] R. Lacey, N.N. Ajitanand, J.M. Alexander, D.M. de Castro Rizzo, G.F. Peaslee, L.C. Vaz, M.Kaplan, M. Kildir, G. La Rana, D.J. Moses, W.E. Parker, D. Logan, M.S. Zisman, P. DeYoung, and L. Kowalski, Phys. Rev. C **37**, 2561 (1988).

[2] J. Boger, J.M. Alexander, R.A. Lacey, and A. Narayanan, Phys. Rev. C **49**, 1587 (1994).

[3] A. Elmaani, Ph.D. thesis, Department of Chemistry, State University of New York at Stony Brook, 1991.

[4] A. Elmaani, N.N. Ajitanand, J.M. Alexander, R. Lacey, S. Kox, E. Liatard, F. Merchez, T. Motobayashi, B. Noren, C. Perrin, D. Rebreyend, Tsan Ung Chan, G. Auger, and S. Groult, Phys. Rev. C **43**, R2474 (1991).

[5] A. Elmaani, J.M. Alexander, N.N. Ajitanand, R.A. Lacey, S. Kox, E. Liatard, F. Merchez, T. Motobayashi, B. Noren, C. Perrin, D. Rebreyend, Tsan Ung Chan, G. Auger, and S. Groult, Phys. Rev. C **49**, 284 (1994).

[6] H. Morgenstern, W. Bohne, W. Galster, K. Grabisch, and A. Kyanowski, Phys. Rev. Lett. **52**, 1104 (1984).

[7] T. Ethvignot, A. Elmaani, N.N. Ajitanand, J.M. Alexander, E. Bauge, P. Bier, L. Kowalski, M.T. Magda, P. Desesquelles, H. Elhage, A. Giorni, D. Heuer, S. Kox, A. Lleres, F. Merchez, C. Morand, D. Rebreyend, P. Stassi, J.B. Viano, S. Benrachi, B. Chambon, B. Cheynis, D. Drain, and C. Pastor, Phys. Rev. C **43**, R2035 (1991).

[8] M.T. Magda, T. Ethvignot, A. Elmaani, J.M. Alexander, P. Desesquelles, H. Elhage, A. Giorni, D. Heuer, S. Kox, A.

Lleres, F. Merchez, C. Morand, D. Rebreyend, P. Stassi, J.B. Viano, F. Benrachi, B. Chambon, B. Cheynis, D. Drain, and C. Pastor, Phys. Rev. C **45**, 1209 (1992).

[9] T. Ethvignot, N.N. Ajitanand, C.J. Gelderloos, J.M. Alexander, E. Bauge, A. Elmaani, R.A. Lacey, P. Desesquelles, H. Elhage, A. Giorni, D. Heuer, S. Kox, A. Lleres, F. Merchez, C. Morand, D. Rebreyend, P. Stassi, J.B. Viano, F. Benrachi, B. Chambon, B. Cheynis, D. Drain, and C. Pastor, Nucl. Phys. **A545**, 347c (1992).

[10] T. Ethvignot, N.N. Ajitanand, J.M. Alexander, E. Bauge, A. Elmaani, L. Kowalski, M. Lopez, M.T. Magda, P. Desesquelles, H. Elhage, A. Giorni, D. Heuer, S. Kox, A. Lleres, F. Merchez, C. Morand, D. Rebreyend, P. Stassi, J.B. Viano, F. Benrachi, B. Chambon, B. Cheynis, D. Drain, and C. Pastor, Phys. Rev. C **46**, 637 (1992).

[11] T. Ethvignot, N.N. Ajitanand, J.M. Alexander, A. Elmaani, C.J. Gelderloos, P. Desesquelles, H. Elhage, A. Giorni, D. Heuer, S. Kox, A. Lleres, F. Merchez, C. Morand, D. Rebreyend, P. Stassi, J.B. Viano, F. Benrachi, B. Chambon, B. Cheynis, D. Drain, and C. Pastor, Phys. Rev. C **47**, 2099 (1993).

[12] T. Ethvignot, J.M. Alexander, A.J. Cole, A. Elmaani, P. Desesquelles, H. Elhage, A. Giorni, D. Heuer, S. Kox, A. Lleres, F. Merchez, C. Morand, D. Rebreyend, P. Stassi, J.B. Viano, F. Benrachi, B. Chambon, B. Cheynis, D. Drain, and C. Pastor, Phys. Rev. C **48**, 618 (1993).

[13] A. Elmaani, J.M. Alexander, N.N. Ajitanand, R.A. Lacey, S. Kox, E. Liatard, F. Merchez, T. Motobayashi, B. Noren, C. Perrin, D. Rebreyend, Tsan Ung Chan, G. Auger, and S. Groult, Phys. Rev. C **48**, 2864 (1993).

[14] M.T. Magda and J.M. Alexander, in *Topics in Atomic and Nuclear Collisions*, edited by B. Remaud (Plenum Press, New York, 1994), p. 97.

[15] C.J. Gelderloos, J.M. Alexander, N.N. Ajitanand, E. Bauge, A. Elmaani, T. Ethvignot, L. Kowalski, R.A. Lacey, M.E. Brandon, A. Giorni, D. Heuer, S. Kox, A. Lleres, A. Menchaca-Rocha, F. Merchez, D. Rebreyend, J.B. Viano, B. Chambon, B. Cheynis, D. Drain, and C. Pastor, Phys. Rev. Lett. **75**, 3082 (1995).

[16] C.J. Gelderloos, Rulin Sun, N.N. Ajitanand, J.M. Alexander, E. Bauge, A. Elmaani, T. Ethvignot, R.A. Lacey, M.E. Brandon, A. Giorni, D. Heuer, S. Kox , A. Lleres, A. Menchaca-Rocha, F. Merchez, D. Rebreyend, J.B. Viano, B. Chambon, B. Cheynis, D. Drain, and C. Pastor, Phys. Rev. C **52**, R2834 (1995).

[17] M.T. Magda, E. Bauge, A. Elmaani, T. Braunstein, C.J. Gelderloos, N.N. Ajitanand, J.M. Alexander, T. Ethvignot, P. Bier, L. Kowalski, P. Désequelles, H. Elhage, A. Giorni, S. Kox, A. Lleres, F. Merchez, C. Morand, P. Stassi, J.B. Benrachi, B. Chambon, B. Cheynis, D. Drain, and C. Pastor, Phys. Rev. C **53**, R1473 (1996).

[18] L. Vaz, J.M. Alexander, and N. Carjan, Z. Phys. A **324**, 331 (1986).

[19] D.J. Moses, Ph.D. thesis, Department of Chemistry, Carnegie-Mellon University, 1986.

[20] M.A. McMahan, G.J. Wozniak, C.M. Lyneis, D.R. Bowman, R.J. Charity, Z. H. Liu, L.G. Moretto, W.L. Kehoe, A.C. Mignerey, and M.N. Namboodiri, Nucl. Instrum. Methods Phys. Res. A **253**, 1 (1986).

[21] L. Winsberg and J.M. Alexander, Phys. Rev. **121**, 518 (1961).

[22] V.E. Viola, Jr., B.B. Back, K.L. Wolf, T.C. Awes, C.K. Gelbke, and H. Breuer, Phys. Rev. C **26**, 178 (1982).

[23] L. Pienkowski, A. Lleres, H. Nifenecker, J. Blachot, J. Crancon, A. Gizon, M. Maurel, and C. Ristori, Z. Phys. A **334**, 315 (1989).

[24] N. Colonna, R.J. Charity, D.R. Bowman, M.A. McMahan, G.J. Wozniak, L.G. Moretto, G. Guarino, A. Pantaleo, L. Fiore, A. Gobbi, and K.D. Hildenbrand, Phys. Rev. Lett. **62**, 1833 (1989).

[25] N.N. Ajitanand, R. Lacey, G.F. Peaslee, E. Duek, and J.M. Alexander, Nucl. Instrum. Methods Phys. Res. A **242**, 111 (1986).

[26] A. Lleres, Ph.D. thesis, Institut des Sciences Nucléaires de Grenoble, 1988.

[27] N.N. Ajitanand and J.M. Alexander, Nucl. Instrum. Methods Phys. Res. A **376**, 213 (1996).